CHEMICAL GEOLOGY
INCLUDING
ISOTOPE GEOSCIENCE

Accretionary orogenesis of the Chinese Altai: Insights from Paleozoic granitoids

Chao Yuan [a,b], Min Sun [b,*], Wenjiao Xiao [c], Xianhua Li [a], Hanlin Chen [d], Shoufa Lin [e], Xiaoping Xia [b], Xiaoping Long [a]

[a] *Key Laboratory of Isotope Geochronology and Geochemistry, Guangzhou Institute of Geochemistry, Chinese Academy of Sciences, Guangzhou 510640, China*
[b] *Department of Earth Sciences, The University of Hong Kong, China*
[c] *State Key Laboratory of Lithospheric Evolution, Institute of Geology and Geophysics, Beijing 100029, China*
[d] *Department of Earth Sciences, Zhejiang University, Hangzhou 310027, China*
[e] *University of Waterloo, Department of Earth Sciences, Waterloo, ON, Canada N2L 3G1*

Abstract

Zircon U–Pb dating and whole-rock major oxide, trace element and Nd–Sr isotope compositions have been determined for four representative granitic intrusions in the SW Chinese Altai, in order to understand the orogenesis and history of crustal growth in the Central Asian Orogenic Belt (CAOB). The Ashile and Halatas bodies are relatively small intrusions formed in the Late Carboniferous (318 ± 6 Ma) and Permian (267 ± 4 Ma), respectively. The larger Tarlang (TB) and Keketuohai Batholiths (KB) have magmatic ages of 359 to 412 Ma. The granitoids consist chiefly of tonalite, granodiorite and granite, and are metaluminous to weakly peraluminous in composition (ASI = 0.8–1.1). The Ashile Pluton is characterized by relatively high MgO (2.73–3.54 wt.%) and Sr (395–456 ppm) contents, with low K_2O/Na_2O ratios (0.31–0.42) and mantle-like Nd–Sr isotopic compositions (εNd_T = +2.85 to +3.26; initial $^{87}Sr/^{86}Sr$ = 0.7047–0.7051). It probably formed by fractional crystallization of a mantle-derived magma, with limited assimilation of old crustal material. The other intrusions have near-zero or negative εNd_T values (−0.67 to −4.41) and higher Sr isotopic compositions (initial $^{87}Sr/^{86}Sr$ = 0.7067–0.7092), indicating a mixture of juvenile and old components in their genesis. These intrusions are characterized by relatively low K, Rb, Cs contents and low Rb/Sr ratios (mostly < 0.6), and generally exhibit moderate to high heavy rare earth element (HREE) concentrations (Yb_N = 8–26) and weak HREE fractionation (Dy/Yb_N < 1.5), with or without negative europium anomalies (Eu/Eu* = 0.5–1.0). These characteristics are consistent with an origin by dehydration melting of a hornblende-bearing, mid-crustal source (above the garnet stability field) dominated by mafic to intermediate rocks. This suggests that the deep crust of the Chinese Altai may contain a considerable proportion of juvenile material. Mantle-derived magmatism, probably in an active extensional continental margin setting, played an important role in the formation of the Chinese Altai, acting not only as a heat source for crustal melting but as a source of juvenile components. The relatively small volumes and distinct geochemical compositions of the Ashile and Halatas Plutons may imply a substantial change in the geodynamic setting in the late Paleozoic.
© 2007 Elsevier B.V. All rights reserved.

Keywords: CAOB; Chinese Altai; Granitoids; Dehydration–melting; Active continental margin; Accretionary orogenesis

---

* Corresponding author. Tel.: +852 2859 2194; fax: +852 2517 6912.
E-mail address: minsun@hku.hk (M. Sun).

1. Introduction

The Central Asian Orogenic Belt (CAOB), also known as the Altaids (Sengör et al., 1993; Sengör and Natal'in, 1996), is one of the largest accretionary orogenic belts in the world. In contrast to the classic collisional orogenic belts formed by amalgamation of two continental blocks (Windley, 1995), the CAOB is characterized by accretion of various terranes, such as ophiolites, accretionary prisms and possibly some microcontinents. It is believed that at least half of its growth was due to the addition of juvenile material, by both lateral and vertical accretion during the Neoproterozoic and Paleozoic (Sengör et al., 1993; Windley et al., 2002; Jahn, 2004a). Understanding the tectonic evolution of the CAOB is important, not only for resolving the amalgamation history of Central Asia, but also for understanding the processes of continental crustal accretion. Several models have been proposed for development of the giant CAOB accretionary collage. Many workers considered that the formation of the CAOB occurred by consumption of small ocean basins (e.g. Dobertsov et al., 1995; Yakubchuk, 2004), whereas Sengör and his colleagues envisaged continuous lateral accretion along the southern margin of the Siberian Craton through oroclinal bending of a single arc chain (Sengör et al., 1993; Sengör and Natal'in, 1996). More recent investigations have revealed, however, that the CAOB contains various terranes indicating a more complex tectonic history (Lamb and Badarch, 2000; Heubeck, 2001; Windley et al., 2002; Khain et al., 2003; Xiao et al., 2003; 2004; Kröner et al., 2005). Records of magmatic and metamorphic events in this orogenic belt can provide valuable information on its origin and evolution but progress in unraveling the tectonic history of the CAOB has been seriously retarded by the lack of reliable age data.

Granitoids are the most important component of continental crust, and their generation, segregation, aggregation and emplacement may be closely related to geodynamic events (Brown, 1994; Solar et al., 1998; Barbarin, 1999; Petford et al., 2000). In addition, the composition of granitic rocks is mainly controlled by their crustal sources and P–T conditions of melting. Thus, granitoids can be used as an important probe for determining their source compositions and petrogenesis (e.g. Rushmer, 1991; Rapp and Watson, 1995; Patiño Douce, 1996, 1999; Haschke and Günther, 2003).

Granitoids make up about 40% of the exposed rock in the Chinese Altai (Zou et al., 1988), and are pivotal to understanding the processes of crustal growth in central Asia (Jahn, 2004a,b). Several previous geochemical studies of the Altai granitoids have attempted to determine the proportion of juvenile material in these rocks, but few systematic geochronological and geochemical studies have been carried out, especially for the calc-alkaline granitoids. Thus, we conducted in situ LA-ICP-MS (Laser ablation-Inductively coupled plasma-Mass spectrometry) zircon U–Pb analyses for representative granitic intrusions along the southeast margin of the Chinese Altai, and determined their whole-rock geochemistry in order to investigate the accretionary process involved in formation of the CAOB.

2. Geological background and the granitic intrusions

The Chinese Altai is located to the northeast of the Junggar basin, and separated from it by the Irtysh Fault (Fig. 1). The geology of this area has been described in detail by previous workers (Windley et al., 2002; Chen and Jahn, 2002; Xiao et al., 2004), thus we only briefly outline the stratigraphy and rock associations. The oldest strata cropping out in the Chinese Altai is the Habahe Group, which consists mainly of terrigenous and volcaniclastic sedimentary rocks with subordinate volcanic rocks. The Habahe Group is dated as Mid- to Late Ordovician based on micropaleoflora (Yu et al., 1995). Recent detrital zircon U–Pb data for clastic rocks from the Habahe Group indicate a maximum depositional age of around 470 Ma (Long et al., 2006). This is consistent with previous interpretations and suggests that the Habahe Group was deposited post Mid-Ordovician. Unconformably overlying the Habahe Group is the Silurian Kulumutu Group, which consists mainly of metaclastic rocks with low- (chlorite–biotite–garnet–staurolite–andalusite–sillimanite–cordierite) or high-grade (garnet–staurolite–kyanite–sillimanite) metamorphic mineral associations (Windley et al., 2002). Resting unconformably on the Early Paleozoic sedimentary rocks is the Early Devonian Kangbutiebao Formation, consisting of volcaniclastic rocks and bimodal lavas (He et al., 1995; Zhang et al., 2000). The overlying Altai Formation is mainly composed of turbidites with mafic to silicic volcanic rocks and was probably formed in a magmatic arc or forearc basin invaded by a migrating magmatic front (Sengör and Natal'in, 1996). The Altai Formation has generally been assigned to the Middle Devonian (Windley et al., 2002), but its precise depositional age is uncertain. Late Devonian strata are missing in this area, and next in the sequence are fine-grained, clastic sedimentary rocks with minor mafic to intermediate volcanic material of Carboniferous age that lie in the eastern part of the mountain range (Fig. 1).
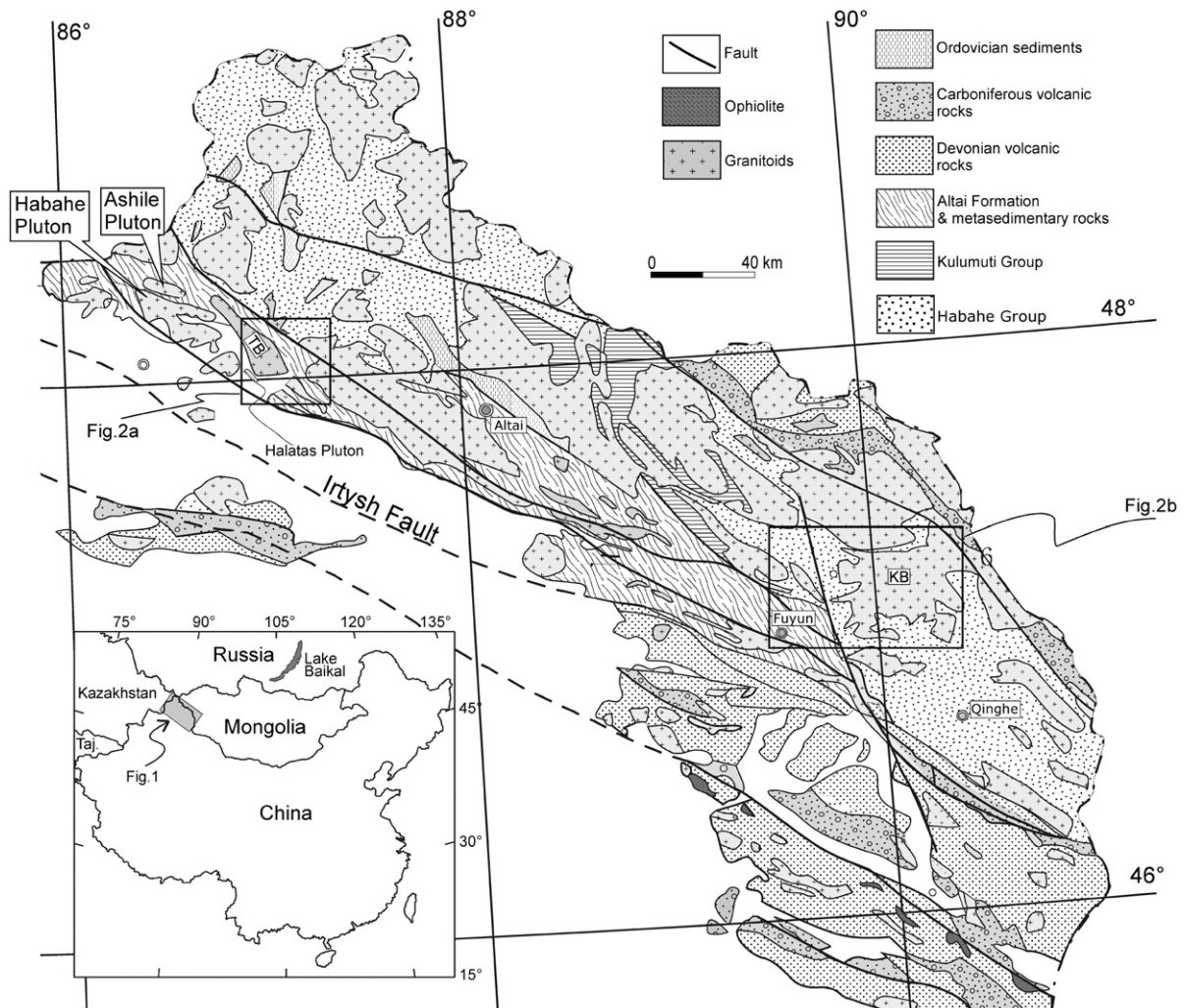
Fig. 1. Geological map of the Chinese Altai.

The Paleozoic rocks have been variably metamorphosed and display inverted metamorphic isograds, with high-grade gneisses thrust southward over weakly metamorphosed rocks (Qu and Zhang, 1994; Windley et al., 2002). Although these meta-sedimentary rocks have traditionally been assigned to the Early Paleozoic, their exact age is not well constrained, especially for those on the south flank of Altai, where intense deformation, high-grade metamorphism and relatively higher Nd model ages have led some workers to suggest these rocks being part of the Early to Middle Proterozoic basement (e.g. Chen and Jahn, 2002).

In this study, four representative granitic intrusions along the southern margin of the Chinese Altai were selected for detailed study; the Ashile Pluton in the west, the Tarlang Batholith (TB) and Halatas Pluton in the middle, and the Keketuohai Batholith (KB) in the east

(Fig. 1). The Ashile Pluton, a small body intruding the Altai Formation, consists of relatively homogeneous granodiorite. The TB contains mostly two-mica granite, locally intruded by biotite granodiorite (Fig. 2a), and variable migmatization of the wallrock and post-intrusive deformation have produced a transitional contact relationship. The small and relatively homogeneous Halatas Pluton is dominated by medium-grained, light gray granodiorite. It also intrudes the Altai Formation but has not been significantly deformed. Recent Ar–Ar dating of hornblende from this pluton yielded ages of 267.1±3.7 Ma (plateau age) and 264.6±4.4 Ma (isochron age) (Yuan et al., 2005), suggesting formation in the Early Permian. The KB intrudes metasedimentary rocks of the Early Paleozoic Habahe Group and consists of medium-grained, two-mica granite in the north and gray biotite granodiorite in the south (Figs. 1 and 2b).
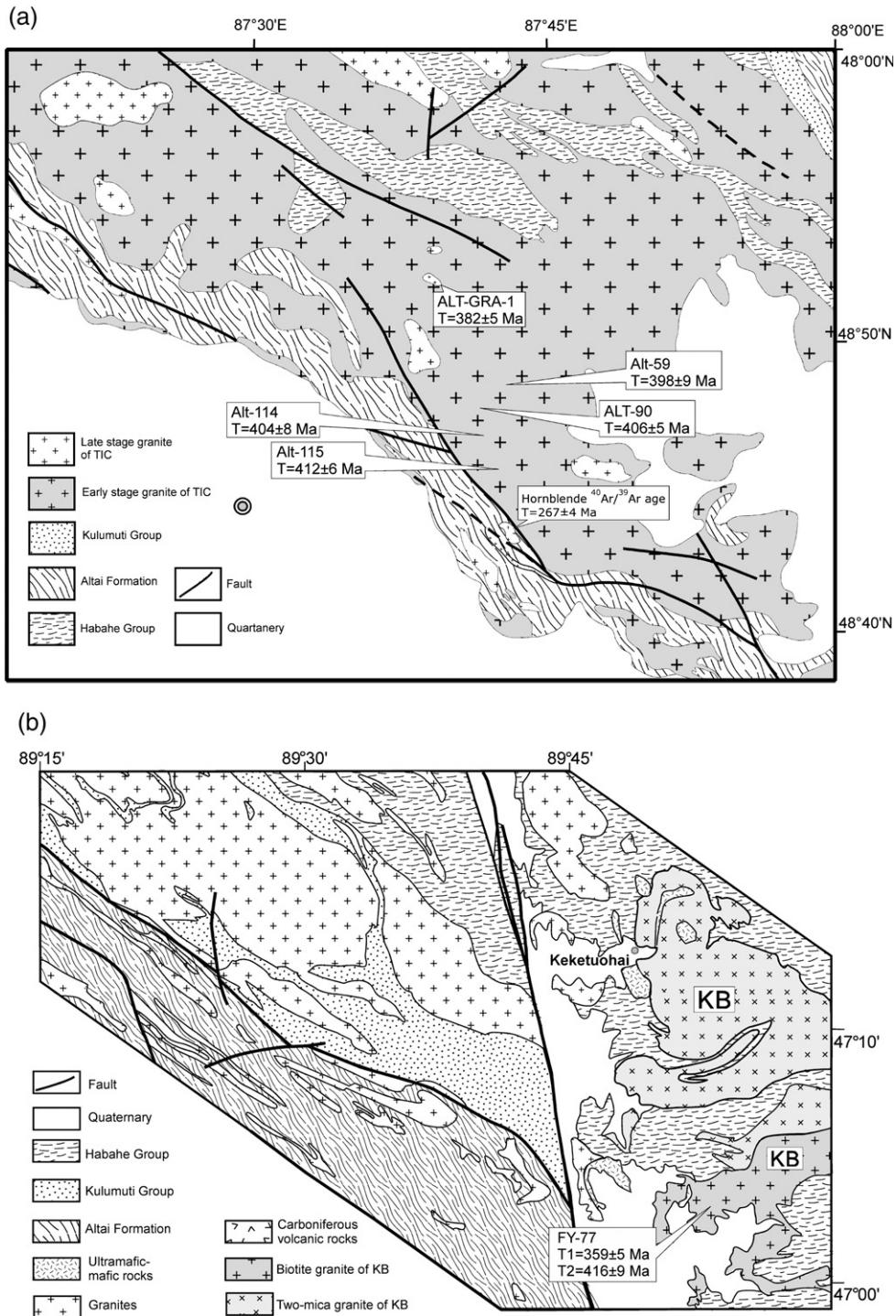
Fig. 2. Geological maps of the Alagake and Keketuohai areas, Chinese Altai. (a) Geological map of the Alagake area. (b) Geological map of the Keketuohai area.

The two-mica granite has not been deformed, whereas the biotite granodiorite locally exhibits a gneissic structure. SHRIMP zircon U–Pb dating yielded an age of

409 ± 7 Ma for the two-mica granite (Wang et al., 2006), whereas Rb–Sr isochron and zircon U–Pb dating yielded ages of 340–360 Ma for the KB gneissic biotite

granodiorite (Kang and Wang, 1992). Massive blocks and enclaves of amphibolite occur both within the TB and the adjacent Habahe Group, and are interpreted as metamorphosed mafic stocks and dykes (Fig. 2b) (Xinjiang Bureau of Geology, 1978).

3. Petrography

The Ashile granodiorite is composed of plagioclase (~50%), hornblende (~30%), biotite (~10%) and quartz (~5%), with minor accessory minerals such as zircon and apatite. Except for quartz, most of the minerals are euhedral, and polysynthetic twinning is well developed in the plagioclase. Small (ca. 1–5 mm), mafic enclaves observed in thin section consist dominantly of plagioclase and hornblende, compositionally similar to those of the host rock. These micro-enclaves are probably fragments of a chilled margin of a magma chamber, representing a previously crystallized pulse of magma (Didier and Barbarin, 1991).

The two-mica granite of the TB is composed of plagioclase, K-feldspar, quartz and mica with variable biotite/muscovite ratios, whereas the gneissic biotite granite of this body consists mainly of plagioclase (~40%), K-feldspar (~20%), biotite (20%), quartz (~20%) and rare hornblende. Accessory minerals, such as zircon, sphene, apatite and allanite, are common in the batholith. The K-feldspar is dominantly orthoclase and microcline. The biotite and muscovite in the rock generally define a weak foliation.

The Halatas Pluton consists of medium- to coarse-grained granodiorite, composed of plagioclase (~50%), hornblende (~15%), biotite (~20%), quartz (~10%) and accessory minerals (zircon, sphene and apatite). These rocks are lithologically similar to the Ashile granodiorite, although they contain more biotite and quartz and less hornblende.

The KB two-mica granite is composed mainly of plagioclase (40%), biotite (15%), muscovite (10%), quartz (15%) and minor K-feldspar (10%). These minerals, except for quartz, are generally euhedral, and are not oriented. The micas generally lie between plagioclase grains, indicating relatively late crystallization. Unlike the two-mica granite, the biotite granodiorite of TB contains minor hornblende and has a good lineation defined by biotite.

4. Analytical methods

Zircon grains were separated by heavy liquids and then hand-picked. Cathodoluminescence (CL) images of the zircon grains were obtained using an electron microprobe (JXA-8100, JEOL) equipped with a Mono CL3 detector (Gatan) at the Guangzhou Institute of Geochemistry, Chinese Academy of Sciences (GIG-CAS). Zircon U–Pb analyses were carried out using an Nd: YAG 213 laser ablation system coupled with a VG Excel ICP-MS at the Department of Earth Sciences, The University of Hong Kong, following the analytical procedure described by Xia et al. (2004). During the analyses, highly purified helium was used as carrier gas to improve the instrumental performance, and zircon standard 91500 was used for calibration. The ablation spot was 30 μm in diameter and no common Pb correction was needed because the ^{204}Pb intensity was much lower than the limit of detection. An intercept method was applied to correct the laser-induced Pb/U fractionation (Sylvester and Ghaderi, 1997) and the ages were calculated using IsoplotEX 4.96 (Ludwig, 2001). Application of the analytical procedure to zircon grains from a syenite intrusion in Yunnan and an alkaline granite in northern Xinjiang yielded $^{206}Pb/^{238}U$ ages of 761±15 Ma and 304±6 Ma, respectively, which are consistent with results obtained by SHRIMP dating (765±9 Ma and 305±7 Ma, respectively). Zircon grains of 7 samples from the TB, KB and Ashile Pluton were analyzed and the results are presented in Table 1. Errors on individual analyses are quoted at 1σ level and those on pooled analyses are quoted at 2σ or 95% confidence level.

Major oxides of selected whole-rock samples were determined with a Philips PW2400 wavelength-dispersive X-ray fluorescence spectrometer (WD-XRFS) on fused glass disks at the University of Hong Kong. Sample powders for trace element analyses were digested with mixed HNO_3+HF acid in steel-bomb coated Teflon beakers in order to assure the complete dissolution of refractory minerals (e.g. zircon). Measurement for trace elements was performed using a VG Elemental Plasma-Quad Excel ICP-MS at the University of Hong Kong. The analytical procedures for the trace element determinations are described in Qi et al. (2000). The analytical precision was better than 2% for major elements and between 5 and 10% for trace elements, depending on the concentration level of a specific element.

Samples for Sm–Nd isotopic analyses were digested in the same way as for trace element analyses. Sr and Nd were separated using a two-step exchange procedure, then $^{87}Sr/^{86}Sr$ and $^{143}Nd/^{144}Nd$ ratios were measured with a Micromass IsoProbe multi-collector mass spectrometer (MC-ICP-MS) at GIGCAS following the procedures described in Wei et al. (2002) and Li et al. (2004). ^{83}Kr, ^{84}Sr, ^{85}Rb, ^{86}Sr, $^{87}(Rb+Sr)$ and ^{88}Sr were simultaneously measured to monitor the interference of ^{84}Kr, ^{86}Kr and ^{87}Rb on Sr isotopes. Kr interference
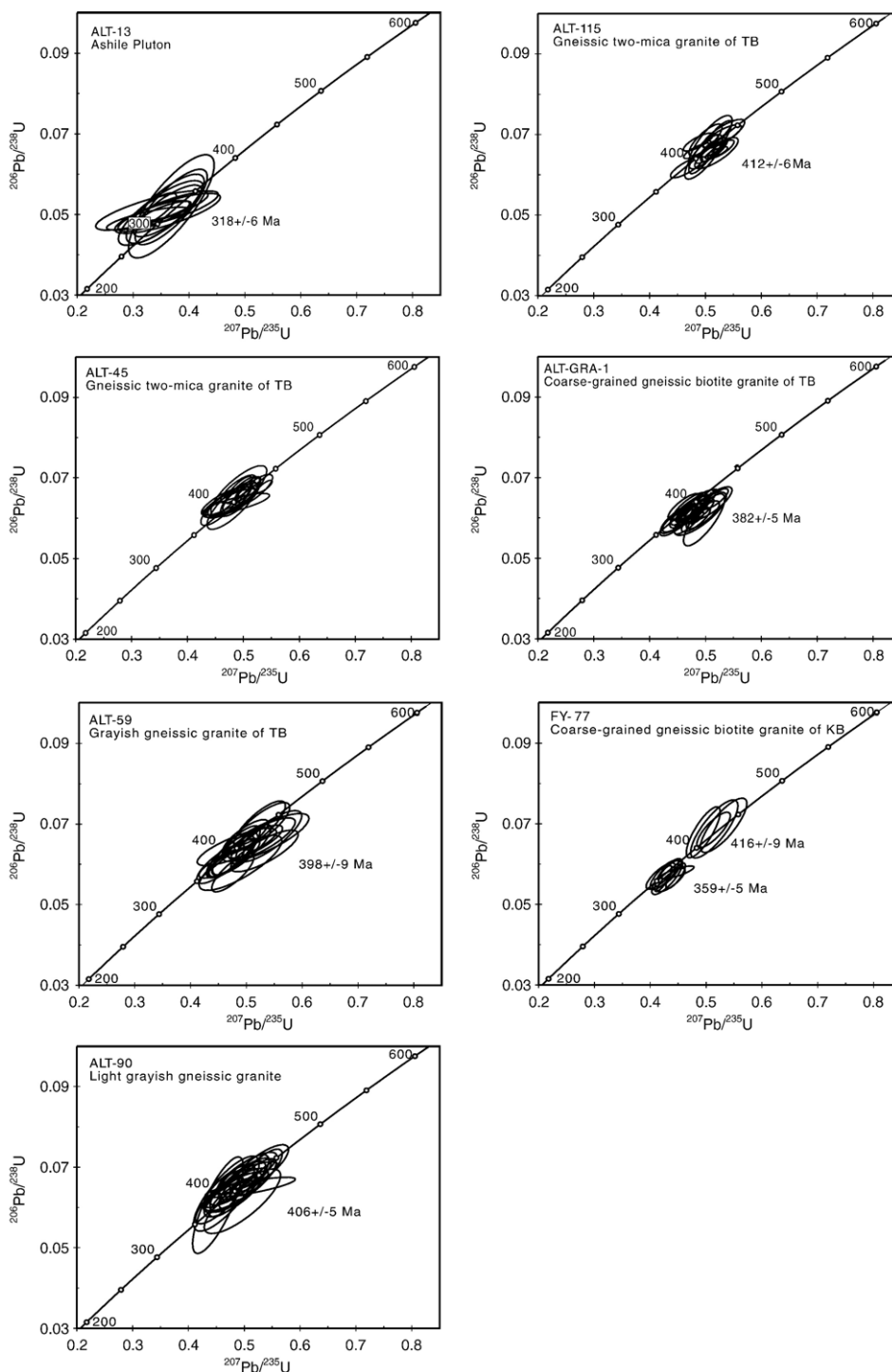
Fig. 3. LA-ICP-MS zircon U–Pb concordia diagrams for the granitic intrusions of the Chinese Altai.

comes predominantly from Ar gas and is generally at a very low level (0.01%) and can be effectively eliminated after blank correction. Interference of ^{87}Rb can be estimated using $^{85}Rb/^{87}Rb = 2.59265$ and a mass fractionation factor calculated based on measured $^{86}Sr/^{88}Sr$ ratios and $^{86}Sr/^{88}Sr = 0.1194$. NBS987 was used as the
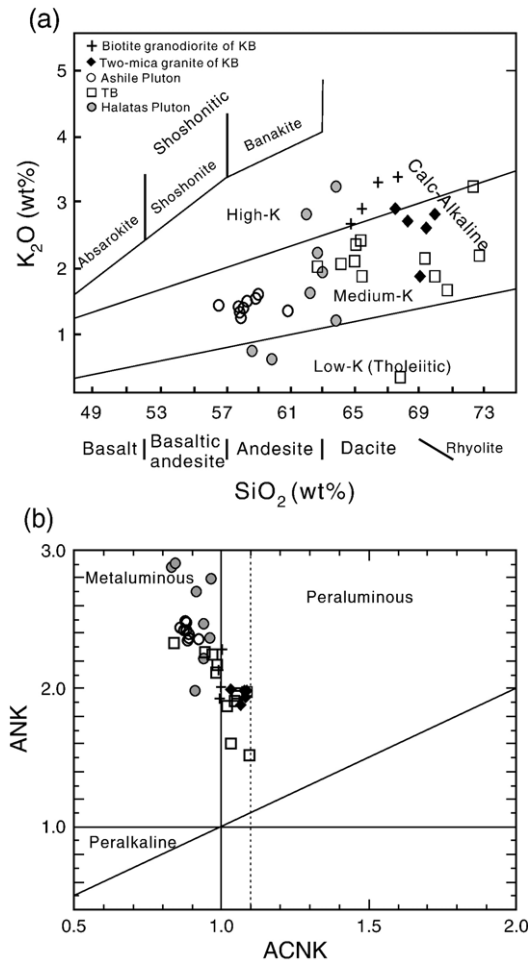
Fig. 4. Chemical classification diagrams for the granitoids of the Chinese Altai. (a) SiO_2 vs K_2O diagram for the granitoids of the Chinese Altai (after Le Maitre et al., 1989). (b) ACNK vs ANK diagram for the granitoids of the Chinese Altai (after Maniar and Piccoli, 1989) (Symbols as in the a).

standard to monitor the instrumental performance for Sr isotope analyses and multiple analyses of NBS987 yielded an average $^{87}Sr/^{86}Sr$ ratio of 0.710247 ± 17 (2σ). Repeated analyses for the Shin Estu JNdi-1 standard during the course of this study yielded an average $^{143}Nd/^{144}Nd$ ratio of 0.512120 ± 8 (2σ). Accordingly, the $^{143}Nd/^{144}Nd$ ratios reported in this study were adjusted relative to the Shin Estu JNdi-1 reference value of 0.512115 (Tanaka et al. 2000), corresponding to the La Jolla standard value (0.511860). The $^{87}Rb/^{86}Sr$ and $^{147}Sm/^{144}Nd$ ratios were calculated from the Rb–Sr and Sm–Nd concentrations determined by the isotope dilution ICP-MS method (Liang et al., 2003). The Nd–Sr isotope data, together with the major and trace element compositions, are shown in Table 2.

5. Analytical results

5.1. Zircon U–Pb results

5.1.1. Ashile Pluton

Zircon grains from the Ashile Pluton are euhedral grains typically with oscillatory zoning or a weak streaky structure. No visible inherited cores were identified. Twelve zircon grains were analyzed and their apparent $^{206}Pb/^{238}U$ ages range from 308 Ma to 327 Ma (Table 1). These analyses form a coherent group with a weighted mean $^{206}Pb/^{238}U$ age of 318 ± 6 Ma (Fig. 3). This age is significantly younger than the 389 Ma Habahe granodiorite in the north (Yuan et al., 2006), and thus represents an independent magmatic event in this region.

5.1.2. Tarlang Batholith (TB)

Several samples of the TB were collected to span its lithological variations. Samples Alt-45 and Alt-115 are gneissic, two-mica granites, and zircon grains from these rocks are generally transparent, euhedral and show oscillatory zoning. Seventeen analyses were conducted for each sample. The analyses of Alt-45 yielded a weighted mean $^{206}Pb/^{238}U$ age of 411 ± 5 Ma, and those from Alt-115 produced a similar age of 412 ± 6 Ma (Fig. 3). Samples Alt-59 and Alt-90 were from medium- to coarse-grained, dark to light gray, gneissic two-mica granite. Zircon grains from these lithologically different samples all show magmatic zoning, and their weighted mean $^{206}Pb/^{238}U$ ages are identical to the other samples within errors, i.e. 398 ± 9 Ma ($n=19$) and 406 ± 5 Ma ($n=20$), respectively (Fig. 3). These results are significantly older than the mid-Devonian age previously assigned to the Altai Formation. Because the Altai Formation is intruded by the TB, it must have been deposited prior to 400 Ma.

Sample ALT-GRA-1 was collected from gneissic biotite granite intruding the dark- to light-gray, gneissic granite of the TB as a later pulse of magma. Zircon grains from this sample are generally euhedral to subhedral without visible inherited cores. Twenty points were analyzed and yielded a weighted mean $^{206}Pb/^{238}U$ age of 382 ± 5 Ma (Fig. 3, Table 1).

5.1.3. Keketuohai Batholith (KB)

Sample FY-77 is from coarse-grained, biotite granodiorite collected in the southern part of the batholith (Fig. 2b). Zircon grains from this sample are euhedral, transparent with oscillatory zoning, and show typical characteristics of magmatic zircon. No inherited cores were observed in the grains. Eighteen grains were analyzed, yielding two age groups. Fourteen analyses

yielded a weighted mean $^{206}Pb/^{238}U$ age of 359 ± 5 Ma that is consistent with a previous zircon U–Pb result (Kang and Wang, 1992), whereas the other analyses yielded a weighted mean $^{206}Pb/^{238}U$ age of 416 ± 9 Ma (Fig. 3).

5.2. Geochemical results

5.2.1. Major element geochemistry

5.2.1.1. The Ashile Pluton. The Ashile Pluton consists of tonalite with intermediate SiO_2 (56.8–61.1 wt.%)

and TiO_2 (0.82–1.02 wt.%) contents and relatively high MgO (2.73–3.54 wt.%). The rocks are metaluminous (ASI = 0.86–0.92) and have medium-K, calc-alkaline characteristics, with K_2O/Na_2O ratios ranging from 0.31 to 0.42 (Fig. 4a, b). In Harker diagrams, most oxides decrease with increasing SiO_2, whereas P_2O_5 remains nearly constant (Fig. 5). On a CIPW-normative ternary diagram, samples from this pluton clearly plot in the tonalite field (Fig. 6).

5.2.1.2. The Tarlang Batholith. This batholith has a wide range of SiO_2 contents (62.8–72.8 wt.%), with low
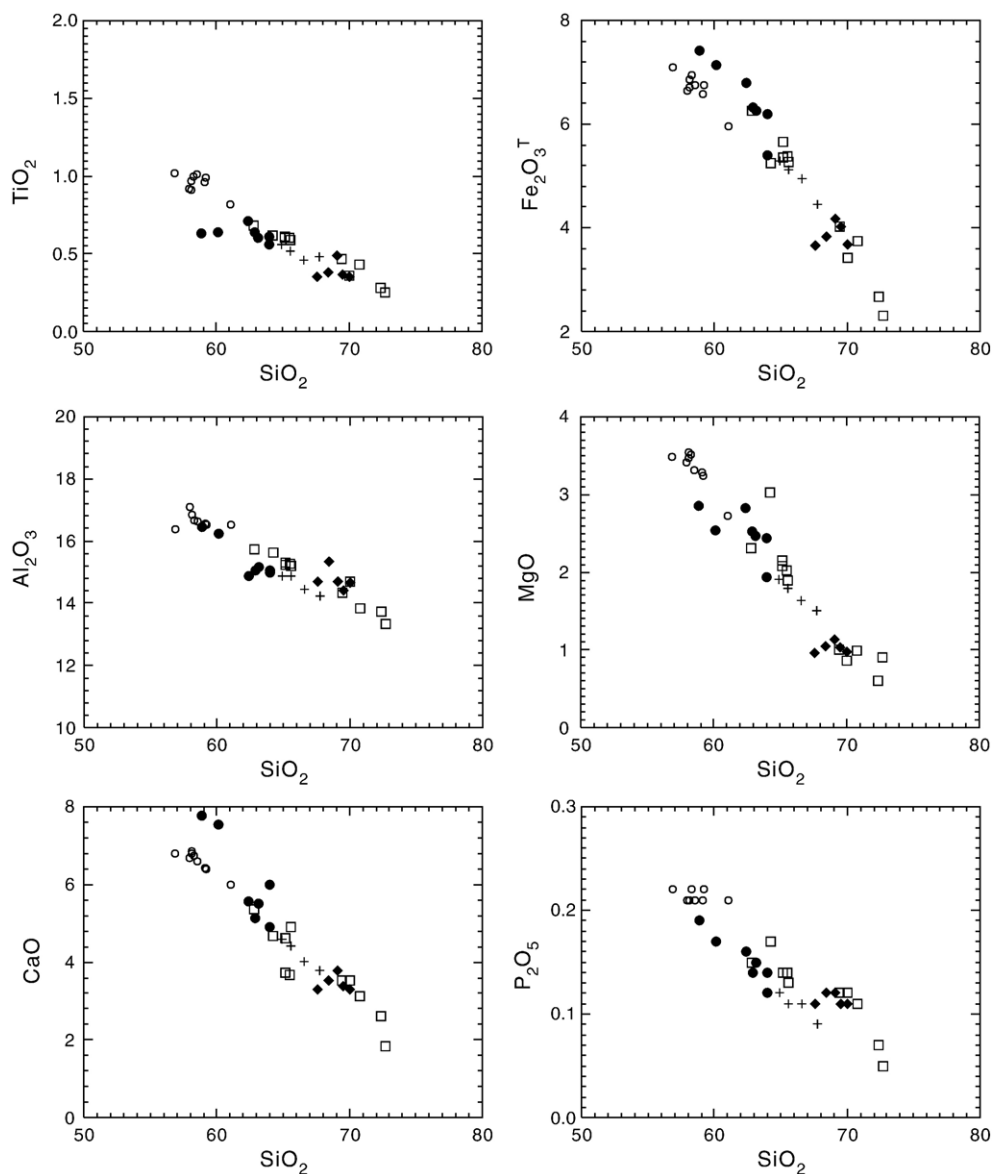

Fig. 5. Major element variation diagrams for the granitoids of the Chinese Altai (symbols as in Fig. 4).

to intermediate TiO_2 (0.25–0.68 wt.%) and MgO (mostly <2.5 wt.%). Samples from this batholith generally have medium-K, calc-alkaline characteristics (Fig. 4a). About half of the samples are slightly peraluminous (1.0< ASI<1.1), whereas the others are generally metaluminous (0.8<ASI<1.0) (Fig. 4b). Although the TB samples are sodium-rich, they have K_2O/Na_2O ratios (0.44–0.65) slightly higher than those of the Ashile Pluton. Most major oxides vary inversely with SiO_2 (Fig. 5). In general, samples from this batholith plot along the boundary between tonalite and granodiorite in the An–Ab–Or classification diagram (Fig. 6).

5.2.1.3. The Halatas Pluton. The HP is metaluminous (ASI=0.83–0.96) and is similar to the Ashile Pluton in composition (Fig. 4a), although it has slightly higher SiO_2 (58.9–64.0 wt.%), and lower TiO_2 (0.60–0.71 wt. %) and MgO (1.93–2.83 wt.%). Because its K_2O contents are variable (0.48–2.55 wt.%), samples from this pluton fall in both the low-K and high-K, calc-alkaline (Fig. 4b) tonalite and granodiorite fields (Fig. 6). Major element compositions for the HP samples also exhibit negative trends with increasing SiO_2 (Fig. 5).

5.2.1.4. The Keketuohai Batholith. The KB consists of two-mica granite and biotite granodiorite. The granite is slightly peraluminous (ASI=1.0–1.1) and shows medium-K calcalkaline characteristics (Fig. 4a). The granodiorite contains lower SiO_2 and slightly higher TiO_2, $Fe_2O_3^T$, CaO and K_2O contents than the granite and has an ASI of ~1 (Fig. 4b). The two rock types

form different variation trends in the Harker diagrams (Fig. 5), but both generally plot in the granodiorite field (Fig. 6).

5.2.2. Trace element geochemistry

5.2.2.1. The Ashile Pluton. The Ashile Pluton contains low Rb (<47 ppm), Cs (<2.4 ppm) and Ba (=190 ppm) but relatively high Sr (395–456 ppm), leading to low Rb/Sr (~0.1) and high Sr/Nd (21–25) ratios (Fig. 7). The samples are characterized by intermediate Nb (5.15–6.51 ppm) and Zr (88–200 ppm) contents, and sub-chondrite Nb/Ta (12–15) and Zr/Hf (35–45) ratios. The rocks of this pluton are relatively depleted in rare earth elements ($\sum$REE<105 ppm) but show light rare earth (LREE) enrichment (La_N/Yb_N=4.7–5.8), negligible HREE fractionation (Dy_N/Yb_N<1.2) and weak europium anomalies (Eu/Eu*=0.8–0.9) in chondrite-normalized patterns (Fig. 8a). In a primitive mantle normalized diagram, samples of the Ashile Pluton show negative Ba, Nb Ta, P, and Ti anomalies and positive Pb and Sr spikes (Fig. 9).

5.2.2.2. The Tarlang Batholith. In comparison with the Ashile Pluton, the TB possesses slightly higher Rb (60.0–91.9 ppm), Cs (1.34–3.86 ppm) and Ba (191–350 ppm) and lower Sr contents (<250 ppm) leading to a higher Rb/Sr ratio (<0.8). There is no significant change of Sr, Rb and Ba with increasing SiO_2 (Fig. 7). The rocks have intermediate Zr (107–274 ppm) and Nb contents (4.07–10.9 ppm) and do not exhibit regular variations with SiO_2 (not shown). Like the Ashile Pluton, the TB exhibits negative Ti, P, Nb, Ta and Ba anomalies and Pb spikes, however, these rocks have negative Sr anomalies that distinguish them from the Ashile Pluton (Fig. 9). Two SiO_2-rich TB samples with relatively low Sr contents are characterized by relatively low Al_2O_3 and larger negative Eu anomalies (Eu/Eu*=0.5), indicating more fractionation of plagioclase. Except for two samples with low HREE, the TB rocks have similar REE patterns (Fig. 8), with intermediate negative Eu anomalies (Eu/Eu*=0.5–0.7). The two HREE-poor samples are characterized by weak Eu anomalies (0.8–1.0), probably indicative of an origin near the garnet stability field.

5.2.2.3. The Halatas Pluton. Although the Halatas Pluton has SiO_2 contents similar to those of the Ashile Pluton (Table 2), it is characterized by relatively low Sr (<250 ppm), and variable Rb (9.36–111 ppm), Cs (0.3–2.2 ppm) and Ba contents (72.6–437 ppm) (Table 2).
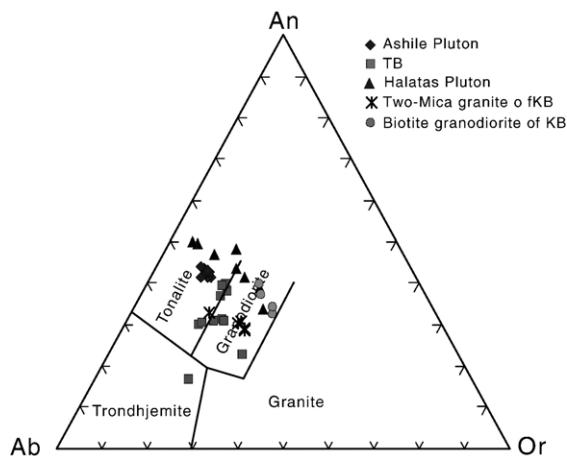

Fig. 6. CIPW-normative ternary diagram for the granitoids of the Chinese Altai (after Barker, 1979).
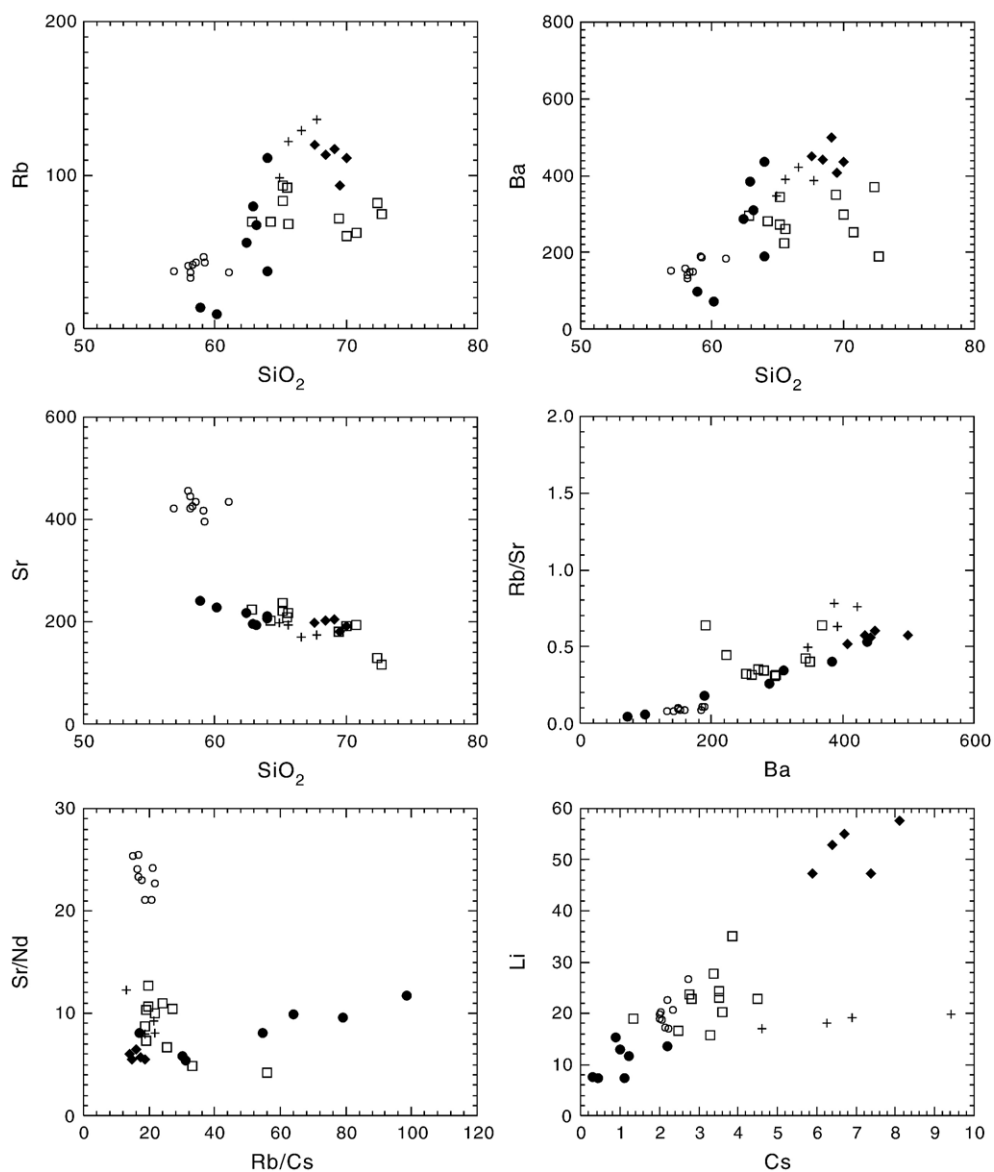
Fig. 7. Trace element variation diagrams for the granitoids of the Chinese Altai (symbols as in Fig. 4).

Samples from the Halatas Pluton have a wide range of Rb/Cs ratios (17–99) that correlate positively with increasing Sr/Nd ratios, a feature distinct from the other intrusions (Fig. 7). The HP samples have LREE-rich chondrite-normalized REE patterns, with unfractionated HREE and intermediate negative Eu anomalies (Eu/ Eu*=0.6–0.7). High field strength element (HFSE) contents are generally in the same range as those of the Ashile Pluton, although most of the trace element patterns are similar to those of the TB, with negative Ba, Sr, P, Nb, Ta and Ti anomalies and Pb spikes (Fig. 9).

5.2.2.4. The Keketuohai Batholith. The KB is characterized by intermediate Sr (<205 ppm), relatively high Rb (98.2–136 ppm), Ba (346–499 ppm), U (1.6– 2.3 ppm), Th (11–16 ppm) and Pb (11–21 ppm) and significantly high Cs contents (4.6–9.4 ppm) (Table 2). The KB two-mica granite contains much higher Li (47– 55 ppm) than does the KB biotite granite (up to 20 ppm) and is characterized by higher Li/Cs ratios (Fig. 7), indicating that the two were probably derived from different sources or experienced a different evolution. Although both the two-mica granite and
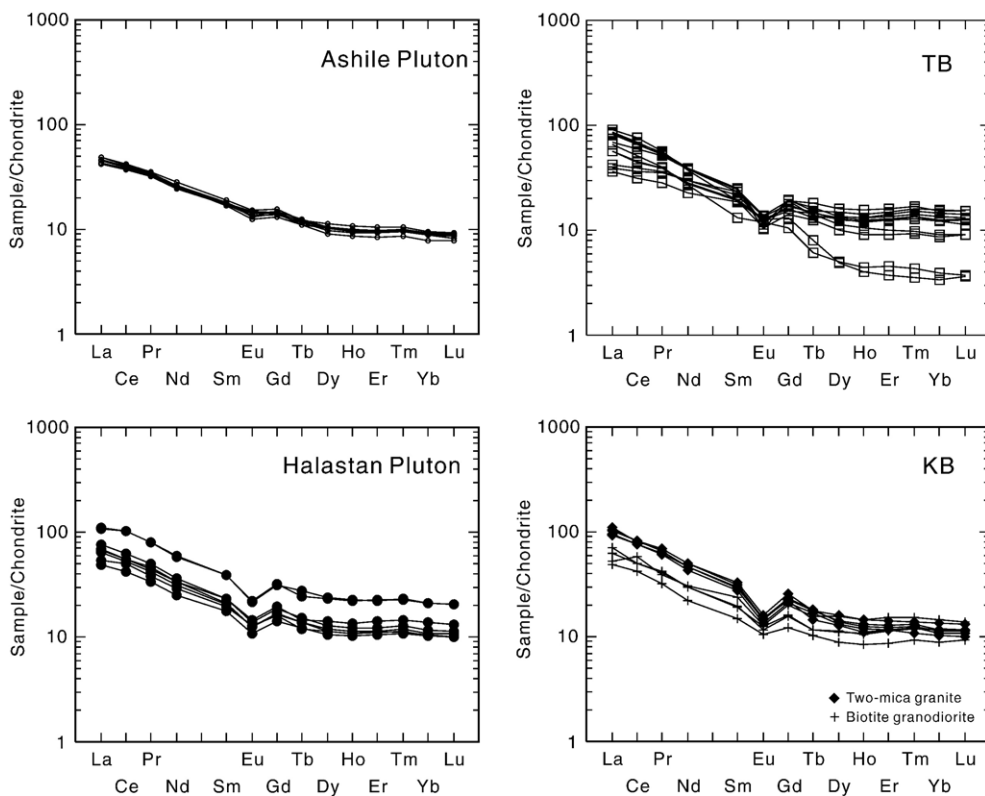
Fig. 8. Chondrite-normalized rare earth element patterns of the granitoids, Chinese Altai (chondrite values are from Taylor and McLennan, 1985).

the biotite granite are LREE-enriched and display similar Eu-anomalies (Eu/Eu*=0.6–0.8), the former is more fractionated (La$_N$/Yb$_N$=7.8–9.7; Dy$_N$/Yb$_N$=1.23–1.30) than the latter (La$_N$/Yb$_N$=3.6–6.0; Dy$_N$/Yb$_N$=~1.0) (Fig. 8). In addition, both rock types exhibit similar trace element patterns that resemble those of the TB (Fig. 9).

5.2.3. Nd–Sr isotope compositions

The Nd–Sr isotopic compositions of the granitoids, together with the calculated initial Sr–Nd isotope compositions, are presented in Table 2. The Ashile Pluton has relatively low initial $^{87}Sr/^{86}Sr$ ratios (0.7047–0.7051), compared to the other granitic intrusions whose ratios vary from 0.7069 to 0.7092 (Table 2, Fig. 10).

The Nd isotope composition of the granitoids is also variable (Table 2, Fig. 10). The Ashile Pluton is the only one with positive εNd$_T$ values (+2.8 to +3.3). The TB and the biotite granite of the KB exhibit slightly negative εNd$_T$ values (−2.7 to −0.7), whereas those of the HP (−4.4 to −2.7) and the two-mica granite of the KB (εNd$_T$=−4.0 to −2.5), are even lower. Despite their different isotopic compositions, the Sm/Nd fraction-

ation of these granitoids is relatively small ($f_{Sm/Nd}$= −0.2–0.4) and well within the range of crustal Sm/Nd (Wu et al., 2000). Therefore, the Nd model ages of the granitoids can be calculated assuming a single-stage linear evolution model (Wu et al., 2000). The Nd model ages of the Ashile Pluton range from 0.91 Ga to 0.95 Ga, whereas other intrusions show older, mid Proterozoic model ages (T_{DM}=1.28–1.89 Ga) (Table 2).

6. Discussion

6.1. Magmatism in the Chinese Altai

Granitoids in the Chinese Altai were considered to be mainly Carboniferous to Cretaceous in age, based on conventional whole-rock Rb–Sr, Sm–Nd isochrone or K–Ar dating (Zhang et al., 1996), and some deformed bodies were thought to represent ancient gneissic terranes (Hu et al., 2000). Our zircon U–Pb results indicate that the TB, regardless of its various degrees of deformation, was emplaced in the Early Devonian (382–412 Ma). Zircons from the coarse-grained biotite granodiorite of the KB yielded ages of 359±5 Ma and 416±9 Ma, which are interpreted to reflect two
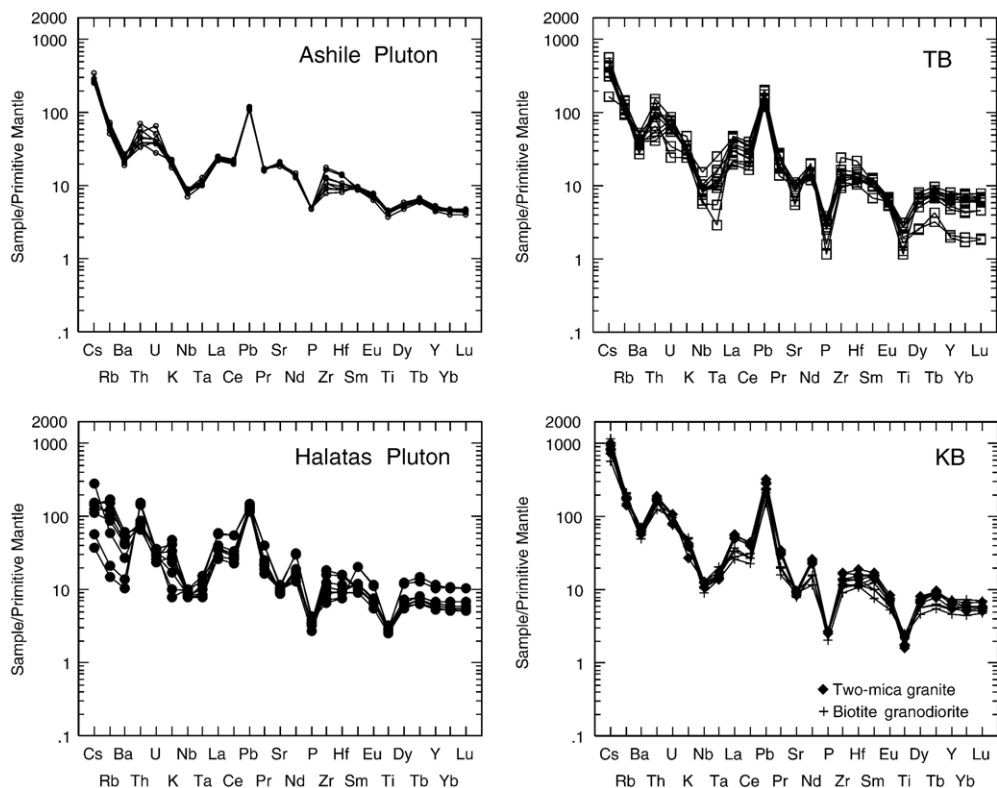
Fig. 9. Primitive mantle-normalized trace element spider diagrams for the granitoids, Chinese Altai (Primitive mantle data are from Sun and McDonough, 1989).

magmatic events. These results, together with recently published data for other areas of the Chinese Altai (370–410 Ma) (Lou, 1997; Zhang et al., 2000; Wang et al., 2006), indicate that Devonian magmatism played an important role in the evolution of the CAOB.

The Ashile Pluton, dated at 318±6 Ma, is the first to be identified of this age in the region, although dikes of similar age have been reported in South Mongolia (Helo et al., 2006). Compared to the Devonian granitoids, late Paleozoic intrusions are sporadic and usually smaller in volume. Because the geochemistry of the Ashile Pluton is consistent with subduction-related magmatism and because previously published data indicate that post-tectonic granitic intrusions in the area were emplaced ca. 300 Ma (Han et al., 1997; Chen and Arakawa, 2005; Su et al., 2006), we suggest that this body was emplaced at 318 Ma in a subduction environment. The unde-formed Halatas Pluton crosscuts lineation in the host rock and has a hornblende $^{40}Ar/^{39}Ar$ age of 267±4 Ma (Yuan et al., 2005), which is similar to the 276±9 Ma zircon U–Pb age reported by Wang et al. (2005) for another post-tectonic granite.

The recent zircon U–Pb dating of granitoids in the Chinese Altai has revealed an almost continuous Paleozoic magmatism, spiking at ca. 500 Ma, 470–460 Ma, 410–380 Ma, 360 Ma and 318–270 Ma (Lou, 1997; Zhang et al., 2000; Yuan et al., 2005; Sun et al., 2006; Long et al., 2006; Wang et al., 2006). These data suggest that the Chinese Altai was located on an active continental margin with continuous subduction at least since the early Cambrian (Sengör and Natal'in, 1996). The small volume and different geochemical composi-tions of the late Paleozoic granitoids may imply a change in the geodynamic environment, probably re-lated to oblique subduction.

6.2. Petrogenesis of the granitoids

6.2.1. The Ashile Pluton

The depleted Nd–Sr isotope composition, relatively young T_{DM} values (<1.0 Ga) and low Sr/Y and high Ba/Nb ratios suggest that the Ashile granodiorite is genetically distinct from the other granitoids studied (Fig. 10). Because no mafic microgranitoid enclaves (MME) have been found in the Ashile Pluton, mixing of mafic and silicic melts seems unlikely. The Nd–Sr isotope composition of the Ashile Pluton suggests that it was derived from a juvenile source and produced either
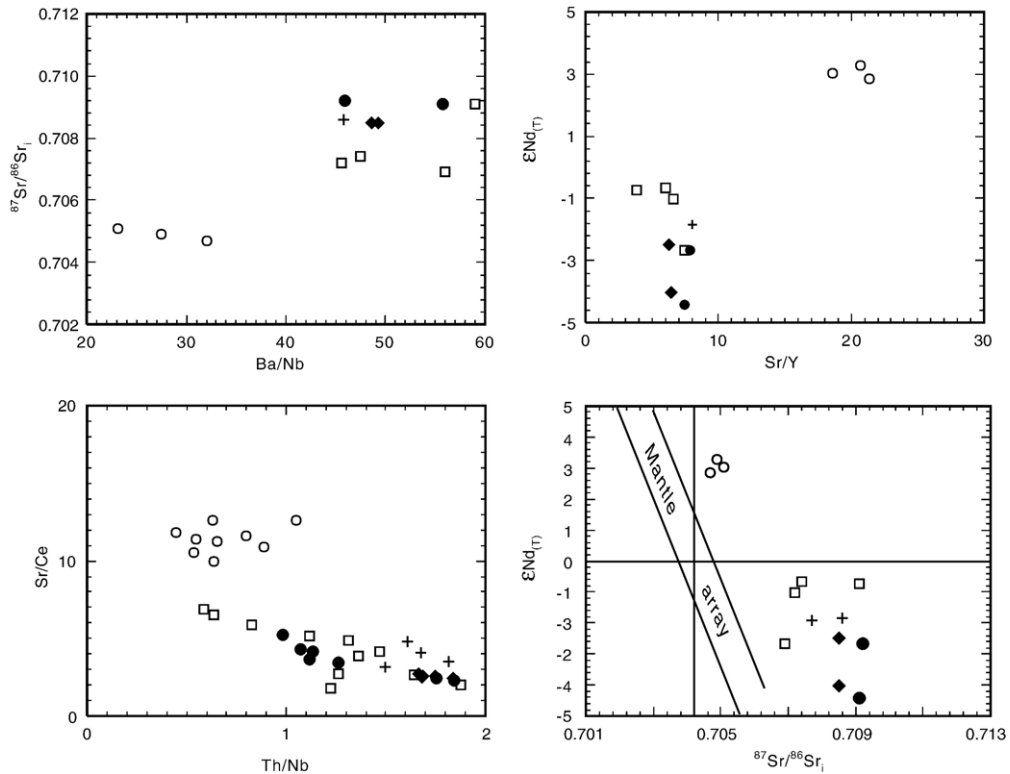
Fig. 10. Incompatible element ratios and initial isotopic composition correlation diagrams. Ba/Nb vs. $^{87}Sr/^{86}Sr$ diagram. Sr/Y vs. εNd_T diagram. Th/Nb vs. Sr/Ce diagram. Correlation diagram between $^{87}Sr/^{86}Sr_i$ and εNd_T. Symbols as in Fig. 4a. See text for explanation.

by differentiation of a mantle-derived magma through AFC processes or by partial melting of juvenile materials. If the Ashile Pluton was generated from partial melting of a mafic source, its relatively high Yb content and flat HREE patterns imply anatexis above the level of the garnet stability field (<10 kb) (Patiño Douce, 1996; Singh and Johannes, 1996). Because of its metaluminous composition, the Ashile Pluton cannot have been formed by H_2O-saturated melting of a mafic source, as melt formed in this way is usually peraluminous (Turpin et al., 1990; Beard and Lofgren, 1991; Patiño Douce and Beard, 1995; Ratajeski et al., 2005). Under mid-level crustal pressures, dehydration melting of metabasaltic or amphibolitic rocks produces melts characterized by high SiO_2 (66–75 wt.%) and low MgO (0.24–1.70 wt.%) contents (Beard and Lofgren, 1991) (Wolf and Wyllie, 1994; Rapp and Watson, 1995; Patiño Douce, 1999). The Ashile Pluton contains intermediate SiO_2 (<62 wt.%) and relatively high MgO (2.7–3.5 wt.%), which is strikingly different from such experimental melts. The Ashile granodiorite has relatively radiogenic Sr isotopic compositions that diverge from the mantle array (Fig. 10), but its relatively homogeneous Nd–Sr isotope composi-

tions preclude significant assimilation of crustal materials. The isotopic compositions are consistent with derivation from subduction-related magmas (Breeding et al., 2004). Although magmatism in the Chinese Altai was waning by the Late Carboniferous, and was dominantly intermediate to silicic in composition (Li et al., 1998), there is geological evidence that the region was still an active continental margin during the late Paleozoic (Sengör et al., 1993; Windley et al., 2002; Xiao et al., 2004). Mafic to intermediate intrusions of the Late Carboniferous in the southern Mongolia and northern Inner-Mongolia are believed to reflect such a tectonic environment (Chen, 2002; Helo et al., 2006).

6.2.2. The TB, HP and KB

The TB, HP and KB are all similar in major and trace element composition (Figs. 5 and 10). They have crustal Nd–Sr isotope signatures ($\varepsilon Nd_T = -4.4$ to -0.7; initial $^{87}Sr/^{86}Sr = 0.7069–0.7092$) (Fig. 10), suggesting that they were not formed directly from mantle-derived magmas. However, their near-zero εNd_T values indicate that they contain both mantle and crustal components. The lack of MME and coeval mafic intrusions imply that

magma mixing or mingling between mantle- and crust-derived melts was not a major process involved in the formation of these granitoids. We consider them to be the products of dehydration melting in the middle and lower crust where the very low porosity of metamorphic rocks prevents large amounts of water from being involved (Clemens and Vielzeuf, 1987; Skjerlie et al., 1993).

The TB, HP and KB possess low $(K_2O+Na_2O)/CaO$ ratios and contain low contents of high field strength elements (HFSE). Their low to intermediate Al_2O_3 (<16.5 wt.%) and Sr (<250 ppm) contents and their mostly negative Eu anomalies (0.5–0.8) can be ascribed to a plagioclase residuum in the source. Hornblende and mica are the most common hydrous minerals involved in dehydration–melting that generates granitic magmas. The relatively low Sr and high HREE (Yb up to 3.92 ppm), together with the weakly fractionated HREE (Fig. 8) and low Sr/Y ratios (mostly less than 20), suggest that these granitoids were mainly derived from a crustal source above the garnet stability field (<10 kb) (Patiño Douce, 1996; Singh and Johannes, 1996). The two TB samples (ALT-32 and ALT-35) with significant depletion of HREE, low Nb and Ta contents (Table 2; Fig. 8c) and weak to nil Eu anomalies (Eu/Eu*=0.8–1.0), probably reflect the presence of garnet and Fe–Ti oxide in the partial melting residue and thus, a relatively deeper origin (Rushmer, 1991; Wyllie and Wolf, 1993).

6.3. Source of the granitoids

Based on the transitional relationship that exists between many of the Altai plutons and their country rock, previous workers suggested that the granitoids
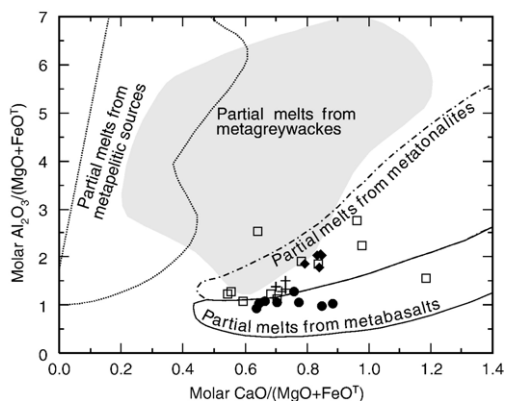

Fig. 11. $Al_2O_3/(MgO+FeO^T)$ vs. $CaO/(MgO+FeO^T)$ diagram for granitoids of the Chinese Altai (after Gerdes et al., 2002) (symbols as in editors">Fig. 4a). FeO^T: total Fe as FeO, calculated from $Fe_2O_3^T/1.111$.

were transformed from their metasedimentary hosts (Zhuang, 1993; Zhao et al., 1993; He et al., 1995). Chen and Jahn (2002) argued that the Nd isotope compositions of the granitoids required a deeper source dominated by juvenile materials. For the granites of the current study, their relatively high TiO_2, $Fe_2O_3^T$, and MgO contents, along with their metaluminous to weakly peraluminous character, preclude their derivation from a pelite source (Vielzeuf and Holloway, 1988; Montel and Vielzeuf, 1997). Their relatively low K, Rb and Cs contents and low K_2O/Na_2O (mostly <1.0) and Rb/Sr (<0.8) ratios (Fig. 7), argue against significant mica in their source. A lack of upwardly-concave, chondrite-normalized REE patterns indicates that amphibole was not a major residual phase during their formation (Borg and Clynne, 1998), consistent with a hornblende dehydration melting reaction.

Hornblende is abundant in mafic to intermediate igneous and metamorphic rocks, and recent experiments and case studies have revealed that significant proportions (25–47 wt.%) of melt can be generated from basaltic or tonalitic sources by dehydration melting (Petcovic and Grunder, 2003; Sisson et al., 2005). Compared to partial melts derived from mica-rich pelite and greywacke, those formed by dehydration melting of amphibolite generally have lower Al_2O_3 and K_2O and higher CaO (Beard and Lofgren, 1991; Rushmer, 1991; Wolf and Wyllie, 1994; Patiño Douce and Beard, 1995; Rapp, 1995; Rapp and Watson, 1995; Gerdes et al., 2002). In the $Al_2O_3/(MgO+FeO^T)$ vs. $CaO/(MgO+FeO^T)$ diagram (Fig. 11), samples of the TB, HP and KB plot dominantly in the fields of meta-igneous sources, suggesting that these rocks were derived mainly by partial melting of metamorphosed mafic to intermediate rocks.

Although the HP samples contain higher MgO (1.93–2.85 wt.%) (Table 2, Fig. 5) than would be expected in a magma (generally <1.0 wt.%) formed by partial melting of metabasaltic materials under relatively low pressures (<10 kb) and temperatures (<1000 °C) (Beard and Lofgren, 1989, 1991; Rapp and Watson, 1995; Skjerlie and Johnston, 1996), their Nd–Sr isotope compositions are similar to those of the TB and KB (Table 2, Fig. 10), suggesting a similar source composition. On variation diagrams, the major oxides, incompatible element ratios and isotopic compositions of all these granitoids form linear trends (Fig. 5; Fig. 10), further implying a similar petrogenesis. Experimental work shows that, at relatively high temperatures (>1000 °C) and intermediate pressures (8 kb), melt from a metabasalt can contain relatively high MgO (up to 3 wt.%) (Beard and Lofgren, 1989, 1991; Rapp and

Watson, 1995), similar to what is observed in the HP. Mafic intrusions of Permian age in the Chinese Altai range (Han et al., 2004; Chen and Han, 2006) may have provided the heat for required partial melting of the middle crust that generated the HP.

We note, however, that partial melting of purely mantle-derived, mafic to intermediate igneous rocks cannot produce magma with strong crustal signatures. The HP, TB and KB possess near-zero εNd_T values, and their wide range of T_{DM} ages (1.28–1.89 Ga) indicate that both juvenile and old continental materials were involved in their genesis. The transitional boundaries of the TB and KB suggest substantial assimilation of the country rock.

6.4. Response to geodynamics of the Chinese Altai

Subduction-related igneous rocks are widely distributed along destructive plate margins, either as intrusions or as materials accreted at relatively shallow crust levels (<8 kb) (e.g. Rushmer, 1991; Matthews et al., 1999). The Chinese Altai was an accretionary margin from Cambrian to Permian, where subduction-related magmatism and accreted ophiolites contributed to crustal growth (Sengör et al., 1993; Sengör and Natal'in, 1996). Because of the relatively high temperatures required for dehydration melting of hornblende, partial melting of newly accreted, mid-crustal mafic to intermediate igneous rocks cannot be achieved through normal crust thickening. Rather, it requires underplating or intraplating of hot mafic magmas to fuse the protolith (Huppert and Sparks, 1988; Petford et al., 2000; Petford and Gallagher, 2001; Barnes et al., 2002). In the Chinese Altai, a bimodal volcanic sequence in the Kangbutiebao Formation and a gabbroic intrusion in the Keketuohai, with ages of 407±9.2 Ma and 405±11 Ma (zircon U–Pb results), respectively (Zhang et al., 2000; Wang et al., 2006), probably reflect intraplating of mantle-derived magma in an extensional setting, as has occurred in Baja California and other accretionary margins (Castillo et al., 2002; Collins, 2002; Busby, 2004). A suite of Mid- to Late Devonian andesites, volcaniclastic rocks and pillow basalts with MORB signatures occurs along the southern margin of the Chinese Altai. These volcanic rocks have been interpreted as the result of decompressional melting of an upwelling asthenospheric mantle (Xu et al., 2003), indicating that extensional environment persisted to the Middle or Late Devonian. The coeval granitoids and bimodal volcanic rocks imply that the mantle-derived magma not only provided heat for anatexis of granitoid protoliths, but also juvenile materials for vertical accretion of the crust.

7. Conclusions

LA-ICP-MS zircon U–Pb dating shows that the Ashile Pluton was emplaced in the Late Carboniferous (318±6 Ma), whereas the TB and KB consist of multiple pulses mainly emplaced in the Devonian (ca. 410–360 Ma). The Altai granitoids consist dominantly of tonalite, granodiorite and granite. Geochemical data suggest that the Ashile Pluton probably formed by fractional crystallization of a mantle-derived magma, whereas the other intrusions were generated by crustal anatexis, most likely by dehydration melting of mid-crustal mafic to intermediate meta-igneous rocks followed by variable assimilation of old crustal materials. Heat for the partial melting of the mid-crustal amphibolites was produced by intraplating of hot, mantle-derived magma, probably in an extensional active continental margin. The relatively small volume and distinct geochemical compositions of the Ashile and Halatas Plutons imply a substantial change in the geodynamic environment in the late Paleozoic.

Acknowledgements

Appendix A. Supplementary data

Supplementary data associated with this article can be found, in the online version, at doi:10.1016/j.chemgeo.2007.02.013.

References

Barbarin, B., 1999. A review of the relationships between granitoid types, their origins and their geodynamic environments. Lithos 46, 605–626.

Barker, F., 1979. Trondhjemite: definition, environment and hypotheses of origin. In: Barker, F. (Ed.), Trondhjemite, Dacite and Related Rocks. Elsevier, Amsterdam, pp. 1–12.

Barnes, C.G., Yoshinobu, A.S., Prestvik, T., Nordgulen, Ø., Karlsson, H.R., Sundvoll, B., 2002. Mafic magma intraplating: anatexis and hybridization in arc crust, Bindal batholith, Norway. Journal of Petrology 43, 2171–2190.

Beard, J.S., Lofgren, G.E., 1989. Effect of water on the composition of partial melts of greenstone and amphibolite. Science 244, 195–197.

Beard, J.S., Lofgren, G.E., 1991. Dehydration melting and water-saturated melting of basaltic and andesitic greenstones and amphibolites at 1, 3 and 6.9 kb. Journal of Petrology 32, 365–401.

Borg, L.E., Clynne, M.A., 1998. The petrogenesis of felsic calc-alkaline magmas from the southernmost Cascades, California: origin by partial melting of basaltic lower crust. Journal of Petrology 39, 1197–1222.

Breeding, C.M., Ague, J.J., Bröcker, M., 2004. Fluid–metasedimentary rock interactions in subduction-zone mélange: implications for the chemical composition of arc magma. Geology 32, 1041–1044.

Brown, M., 1994. The generation, segregation, ascent and emplacement of granite magma: the migmatite-to-crustally-derived granite connection in the thickened orogens. Earth-Science Reviews 36, 83–130.

Busby, C., 2004. Continental growth at convergent margins facing large ocean basins: a case study from Mesozoic convergent-margin basins of Baja California, Mexico. Tectonophysics 392, 241–277.

Castillo, P.R., Hawkins, J.W., Lonsdale, P.F., Hilton, D.R., Shaw, A.M., Glascock, M.D., 2002. Petrology of Alarcon Rise lavas, Gulf of California: Nascent intracontinental ocean crust. Journal of Geophysical Research-Solid Earth 107 (B10) AR 2222 DI ARTN 2222.

Chen, B., 2002. Characteristics and genesis of the Bayan Bold Pluton in the southern Sonid Zuoqi, Inner Mongolia: typical island arc magma instead of adakitic rocks. Geological Review 48, 261–266.

Chen, B., Jahn, B.M., 2002. Geochemical and isotopic studies of the sedimentary and granitic rocks of the Altai orogen of northwest China and their tectonic implications. Geological Magazine 139, 1–13.

Chen, B., Arakawa, Y., 2005. Elemental and Nd–Sr isotopic geochemistry of granitoids from the West Junggar foldbelt (NW China), with implications for Phanerozoic continental growth. Geochimica et Cosmochimica Acta 69, 1307–1320.

Chen, L.H., Han, B.F., 2006. Geochronology, geochemistry and Sr-Nd-Pb isotopic composition of mafic intrusive rocks in Wuqiagou area, north Xinjiang: constraints for mantle sources and deep processes. Acta Petrologica Sinica 22, 1201–1214 (in Chinese with English abstract).

Clemens, J.D., Vielzeuf, D., 1987. Constraints on melting and magma production in the crust. Earth and Planetary Science Letters 86, 287–306.

Collins, W.J., 2002. Hot orogens, tectonic switching, and creation of continental crust. Geology 30, 535–538.

Didier, J., Barbarin, B., 1991. The different types of enclaves in granites — nomenclature. In: Didier, J., Barbarin, B. (Eds.), Enclaves and Granite Petrology. Elsevier, Amsterdam, pp. 19–23.

Dobertsov, N.L., Berzin, N.A., Buslov, M.M., 1995. Opening and tectonic evolution of the Paleo-Asian Ocean. International Geology Review 37, 335–360.

Gerdes, A., Montero, P., Bea, F., Fershater, G., 2002. Peraluminous granites frequently with mantle-like isotope compositions: the continental-type Murzinka and Dzhabyk batholiths of the eastern Urals. International Journal of Earth Sciences 91, 3–19.

Han, B.F., Ji, J.Q., Song, B., Chen, L.H., Li, Z., 2004. SHRIMP zircon U-Pb ages of kalatongke No. 1 and Huangshandong Cu-Ni-bearing mafic-ultramafic complexes, North Xinjiang, and geological implications. Chinese Science Bulletin 49, 2424–2429.

Han, B.F., Wang, S.G., Jahn, B.M., Hong, D.W., Kagami, H., Sun, Y.L., 1997. Depleted-mantle source for the Ulungar River A-type granites from Xinjiang, China: geochemistry and Nd–Sr isotopic evidence, and implications for Phanerozoic crustal growth. Chemical Geology 138, 135–159.

Haschke, M., Günther, A., 2003. Balancing crustal thickening in arcs by tectonic vs. magmatic means. Geology 31, 933–936.

He, G.Q., Liu, D.Q., Li, M.S., Tang, Y.L., Zhou, R.H., 1995. The five-stage model of crustal evolution and metallogenic series of chief orogenic belts in Xinjiang. Xinjiang Geology 13, 99–194 (in Chinese with English abstract).

Helo, C., Hegner, E., Kröner, A., Badarch, G., Tomurtogoo, O., Windley, B.F., Dulski, P., 2006. Geochemical signature of Paleozoic accretionary complexes of the Central Asian Orogenic Belt in South Mongolia: constraints on arc environments and crustal growth. Chemical Geology 227, 236–257.

Heubeck, C., 2001. Assembly of Central Asia during the middle and late Paleozoic. In: Hendrix, M.S., Davis, G.A. (Eds.), Paleozoic and Mesozoic Tectonic Evolution of Central and Eastern Asia. Geological Society of America memoirs, vol. 194, pp. 1–22.

Hu, A., Jahn, B.M., Zhang, G., Chen, Y., Zhang, Q., 2000. Crustal evolution and Phanerozoic crustal growth in northern Xinjiang: Nd isotopic evidence. Part I. Isotopic characterization of basement rocks. Tectonophysics 328, 15–51.

Huppert, H.E., Sparks, R.S.J., 1988. The generation of granitic magmas by intrusion of basalt into continental crust. Journal of Petrology 29, 599–624.

Jahn, B.M., 2004a. The central Asian Orogenic Belt evolution and growth of the continental crust in the Phanerozoic. In: Malpas, J., Fletcher, C.J.N., Ali, J.R., Aichison, J.C. (Eds.), Aspects of the Tectonic Evolution of China. Geological Society, London, Special Publications, vol. 226, pp. 73–100.

Jahn, B.M., Capdevila, R., Liu, D.Y., Vernon, A., Badarch, G., 2004b. Sources of Phanerozoic granitoids in the transect Bayanhongor-Ulaan Baatar, Mongolia: geochemical and Nd isotopic evidence, and implications for Phanerozoic crustal growth. Journal of Asian Earth Sciences 23, 629–653.

Kang, X., Wang, S.Z., 1992. Characteristics of granites in Koktokay region, Xinjiang. Acta Petrologica Sinica 8, 399–404 (in Chinese with English abstract).

Khain, E.V., Bibikova, E.V., Salnikova, E.B., Kröner, A., Gibsher, A.S., Didenko, A.N., Degtyarev, K.E., Fedotova, A.A., 2003. The Palaeo-Asian ocean in the Neoproterozoic and early Paleozoic: new geochronologic data and palaeotectonic reconstructions. Precambrian Research 122, 329–358.

Kröner, A., Windley, B.F., Badarch, G., Tomurtogoo, O., Hegner, E., Liu, D.Y., Wingate, M.T.D., 2005. Accretionary growth in the Central Asian Orogenic Belt of Mongolia during the Neoproterozoic and Palaeozoic and comparison with the Arabian–Nubian Shield and the present Southwest Pacific. Geophysical Research Abstracts 7, 06650 SRef-ID: 1607-7962/gra/EGU05-A-06650.

Lamb, M.A., Badarch, G., 2000. Paleozoic sedimentary Basin and volcanic arc systems if southern Mongolia: new stratigraphic and sedimentologic constraints. In: Ernst, W.G., Coleman, R.G. (Eds.), Tectonic Studies of Asia and the Pacific Rim. Bell-wether Publishing Ltd for the Geological Society of America, pp. 107–141.

Le Maitre, R.W., Bateman, P., Dudek, A., Keller, J., Le Bas, M.J., Sabine, P.A., Schmid, R., Sorensen, H., Streckeisen, A., Woolley, A.R., Zanettin, B., 1989. A Classification of Igneous Rocks and Glossary of Terms. Blackwell, Oxford.

Li, H.Q., Xie, C.F., Chang, H.L., Cai, H., Zhu, J.P., Zhou, S., 1998. Study on Metallogenetic Chronology of Nonferrous and Precious Metallic Pre Deposits in North Xinjiang, China. Geological Publication House, Beijing.

Li, X.H., Liu, D.Y, Sun, M., Li, W.X., Liang, X.R., Liu, Y., 2004. Precise U–Pb and Sm–Nd isotopic dating of the supergiant Shizhuyuan polymetallic deposit and its host granite, SE China. Geological Magazine 141, 225–231.

Liang, X.R., Wei, G.J., Li, X.H., Liu, Y., 2003. Precise measurement of ^{143}Nd/^{144}Nd and Sm/Nd ratios using multiple collectors inductively coupled plasma spectrometry (MC-ICPMS). Geochimica 32, 91–96 (in Chinese with English abstract).

Long, X.P., Sun, M., Yuan, C., Xiao, W.J., Wu, F.Y., Xia, X.P., Cai, K.D., 2006. The early Paleozoic sedimentary environment and tectonic evolution in the Chinese Altai: evidence from U–Pb ages and Hf isotopic composition of detrital zircons. The Third National Petrology and Geodynamics Meeting of China, Abstract, pp. 232–233 (in Chinese).

Lou, F.S., 1997. Characteristics of Late Caledonian granites in the Nuerte area, Altay. Jiangxi Geology 11, 60–66 (in Chinese with English abstract).

Ludwig, K.R., 2001. Users manual for a Geochronological Toolkit for Microsoft Excel. Berkeley Geochronology Center. Special Publication, vol. 1a, p. 59.

Maniar, P.D., Piccoli, P.M., 1989. Tectonic discrimination of granitoids. Geological Society of America Bulletin 101, 635–643.

Matthews, S.J., Sparks, R.S.J., Gardeweg, M.C., 1999. The Piedras Grandes-Soncor eruptions, Lascar Volcano, Chile; evolution of zoned magma chamber in the central Andean upper crust. Journal of Petrology 40, 1891–1919.

Montel, L.M., Vielzeuf, D., 1997. Partial melting of metagreywackes, part II. Compositions of minerals and melts. Contributions to Mineralogy and Petrology 128, 176–196.

Patiño Douce, A., Beard, J.S., 1995. Dehydration–melting of biotite and quartz amphibolite from 3 to 15 kb. Journal of Petrology 36, 707–738.

Patiño Douce, A.E., 1996. Effects of pressure and H$_2$O content on the compositions of primary crustal melts. Transactions of the Royal Society of Edinburgh. Earth Science 87, 11–21.

Patiño Douce, A.E., 1999. What do experiments tell us about the relative contributions of crust and mantle to the origin of granitic magmas? In: Carstro, A., Fernandez, C., Vigneresse, J.L. (Eds.), Understanding Granites: Integrating New and Classic Techniques. Geological Society, London, Special Publications, vol. 168, pp. 55–75.

Petcovic, H.L., Grunder, A.L., 2003. Texture and thermal history of partial melting in tonalitic country rock at the margin of a basalt dike, Wallowa Mountains, Oregon. Journal of Petrology 44, 2287–2312.

Petford, N., Cruden, A.R., McCaffrey, K.J.W., Vigneresse, J.L., 2000. Granite magma formation, transport and emplacement in the Earth's crust. Nature 408, 669–673.

Petford, N., Gallagher, K., 2001. Partial melting of mafic (amphibolitic) lower crust by periodic influx of basaltic magma. Earth and Planetary Science Letters 193, 483–499.

Qi, L., Hu, J., Gregorie, D.C., 2000. Determination of trace elements in granites by inductively coupled plasma mass spectrometry. Talanta 51, 507–513.

Qu, G., Zhang, J., 1994. Oblique thrust systems in the Altay orogen, China. Journal of Southeast Asian Earth Sciences 9, 277–287.

Rapp, R.B., 1995. Amphibole-out phase boundary in partially melted metabasalt, its control over liquid fraction and composition, and source permeability. Journal of Geophysical Research 100 (15), 601–615.

Rapp, R.P., Watson, E.B., 1995. Dehydration of metabasalt at 8–32 kbar: implications for continental growth and crust–mantle recycling. Journal of Petrology 36, 891–931.

Ratajeski, K., Sisson, T.W., Glazner, A.F., 2005. Experimental and geochemical evidence for dehydration of the El Capitan Granite, California, by partial melting of hydrous gabbroic lower crust. Contributions to Mineralogy and Petrology 149, 713–734.

Rushmer, T., 1991. Partial melting of two amphibolites: contrasting experimental results under fluid-absent conditions. Contributions to Mineralogy and Petrology 107, 41–59.

Sengör, A.M.C., Natal'in, B.A., 1996. Turkic-type orogeny and its role in the making of the continental crust. Annual Review Earth and Planetary Science 24, 263–337.

Sengör, A.M.C., Natal'in, B.A., Burtman, V.S., 1993. Evolution of the Altaid tectonic collage and Paleozoic crustal growth in Eurasia. Nature 364, 299–307.

Singh, J., Johannes, W., 1996. Dehydration melting of tonalites. Part 1. Beginning of melting. Contributions to Mineralogy and Petrology 125, 16–25.

Sisson, T.W., Ratajeski, K., Hankins, W.B., 2005. Voluminous granitic magmas from common basaltic sources. Contributions to Mineralogy and Petrology 148, 635–661.

Skjerlie, K.P., Patiño Douce, A.E., Johnston, A.D., 1993. Fluid absent melting of a layered crustal protolith — implications for the generation of anatectic granites. Contributions to Mineralogy and Petrology 114, 365–378.

Solar, G.S., Pressley, R.A., Brown, M., Tucker, R.D., 1998. Granite ascent in convergent orogenic belts: testing a model. Geology 26, 711–714.

Su, Y.P., Tang, H.F., Hou, G.S., Liu, C.Q., 2006. Geochemistry of aluminous A-type granites along Dalabut tectonic belt in West Junggar, Xinjiang. Geochimica 35, 55–67.

Sun, S.S., McDonough, W.F., 1989. Chemical and isotopic systematics of oceanic basalts: implications for mantle composition and processes. In: Saunders, A.D., Norry, M.J. (Eds.), Magmatism in the Ocean Basin. Geological Society Special Publication, vol. 42. Blackwell Scientific Publications, pp. 313–346.

Sun, M., Yuan, C., Xiao, W.J., Long, X.P., Xia, X.P., Lin, S.F., 2006. Zircon U–Pb ages of granitic gneisses and intrusions in the Central Terrane of the Chinese Altai Orogen and tectonic implications. Symposium on Continental Growth and Orogeny in Asia (abstract), pp. 99–100.

Sylvester, P.J., Ghaderi, M., 1997. Trace element analyses of scheelite by excimer laser ablation inductively coupled plasma mass spectrometry (ELA-ICP-MS) using a synthetic silicate glass standard. Chemical Geology 141, 49–65.

Tanaka, T., Togashi, S., Kamioka, H., Amakawa, H., Kagami, H., Hamamoto, T., Yuhara, M., Orihashi, Y., Yoneda, S., Shimizu, H., Kunimaru, T., Takahashi, K., Yanagi, T., Nakano, T., Fujimaki, H., Shinjo, R., Asahara, Y., Tanimizu, M., Dragusanu, C., 2000. JNdi-1: a neodymium isotopic reference in consistency with LaJolla neodymium. Chemical Geology 168, 279–281.

Taylor, S.R., McLennan, S.M., 1985. The Continental Crust: its Composition and Evolution. Blackwell, Oxford.

Turpin, L., Cuney, M., Friedrich, M., Bouchez, J.L., Aubertin, M., 1990. Meta-igneous origin of Hercynian peraluminous granites in N. W. French Massif Central: implications for crustal history reconstructions. Contributions to Mineralogy and Petrology 104, 163–172.

Vielzeuf, D., Holloway, J.R., 1988. Experimental determination of the fluid-absent melting relations in the pelitic system. Contributions to Mineralogy and Petrology 98, 257–276.

Wang, T., Hong, D.W., Tong, Y., Hang, B.F., Shi, Y.R., 2005. Zircon U–Pb SHRIMP age and Origin of Post orogenic Lamazhao granitic pluton from Altai orogen: its implications for vertical continental growth. Acta Petrologica Sinica 21, 640–650.

Wang, T., Hong, D.W., Jahn, B.M., Tong, Y., Wang, Y.B., Hang, B.F., Wang, X.X., 2006. Timing, Petrogenesis, and setting of Paleozoic synorogenic intrusions from the Altai Mountains, Northwest China: implications for the Tectonic evolution of an Accretionary orogen. Journal of Geology 114, 735–751.

Wei, G.J., Liang, X.R., Li, X.H., Liu, Y., 2002. Precise measurement of Sr isotope composition of liquid and solid base using (LP) MC-ICPMS. Geochimica 31, 295–299.

Windley, B.F., 1995. The Evolving Continents, 3rd ed. Wiley, Chichester. 526 pp.

Windley, B.F., Kröner, A., Guo, J.H., Qu, G.S., Li, Y.Y., Zhang, C., 2002. Neoproterozoic to Paleozoic geology of the Altai orogen, NW China: new zircon age data and tectonic evolution. Journal of Geology 110, 719–737.

Wolf, M.B., Wyllie, P.J., 1994. Dehydration–melting of amphibolite at 10 Kbar: the effect of temperature and time. Contributions to Mineralogy and Petrology 115, 369–383.

Wu, F.Y., Jahn, B.M., Wilde, S., Sun, D.Y., 2000. Phanerozoic crustal growth: U–Pb and Sr–Nd isotopic evidence from the granites in the northern China. Tectonophysics 328, 89–113.

Wyllie, P.J., Wolf, M.B., 1993. Amphibolite dehydration-melting: sorting out the solidus. In: Prichard, H.M., Alabaster, T., Harris, N.B.W., Neary, C.R. (Eds.), Magmatic Processes and Plate Tectonics. Geological Society, London, Special Publications, vol. 76, pp. 405–416.

Xia, X.P., Sun, M., Zhao, G.C., Li, H.M., Zhou, M.F., 2004. Spot zircon U–Pb isotope analyses by ICP-MS coupled with a frequency quintupled (213 nm) Nd-YAG laser system. Geochemical Journal 38, 191–200.

Xiao, W.J., Windley, B.F., Badararch, G., Sun, S., Li, J., Qin, K., Wang, Z., 2004. Paleozoic accretionary and convergent tectonics of the southern Altaids: implications for the growth of central Asia. Journal of the Geological Society, London 161, 339–342.

Xiao, W.J., Windley, B.F., Hao, J., Zhai, M.G., 2003. Accretion leading to collision and the Permian Solonker suture, Inner Mongolia, China: termination of the central Asian orogenic belt. Tectonics 22, 1014. doi:10.1029/2002TC001396.

Xinjiang Bureau of Geology, 1978. Notes for Geological Map of the Fuyun Area (1:200,000), pp. 94–115.

Xu, J.F., Castillo, P.R., Chen, F.R., Niu, H.C., Yu, X.Y., Zhen, Z.P., 2003. Geochemistry of late Paleozoic mafic igneous rocks from the Kuerti area, Xinjiang, northwest China: implications for backarc mantle evolution. Chemical Geology 193, 137–154.

Yakubchuk, A., 2004. Architecture and mineral deposit settings of the Altaid orogenic collage: a revised model. Journal of Asian Earth Sciences 23, 761–779.

Yu, X.Y., Mei, H.J., Jiang, F.Z., Luo, C.R., Liu, T.G., Bai, Z.H., Yang, X.C., Wang, J.D., 1995. The Irtysh Volcanic Rocks and their Mineralization Processes. Science Press, Beijing.

Yuan, C., Sun, M., Xiao, W.J., Li, X.H., Lin, S.F., Xia, X.P., Long, X.P., Cai, K.D., 2006. Paleozoic Accretion of Chinese Altai: Geochronological Constraints from Granitoids. Abstract of Western Pacific Geophysics Meeting, CD-ROM. Beijing, China.

Yuan, C., Sun, M., Xiao, W.J., Li, X.H., Lin, S.F., Xia, X.P., Long, X.P., Cai, K.D., 2005. Geochronology and Geochemistry of granitoids in the south margin of Chinese Altai. Abstract of Symposium of Petrology and Geodynamics. Hangzhou, China, pp. 219–418.

Zhang, J.H., Wang, J.B., Ding, R.F., 2000. Characteristics and U–Pb ages of zircon in metavolcanics from the Kangbutiebao Formation in the Altay region, Xinjiang. Regional Geology of China 19, 281–287 (in Chinese with English abstract).

Zhang, X.B., Sui, J.X., Li, Z.C., Liu, W., Yang, X.Y., Liu, S.S., Huang, H.Y., 1996. Tectonic Evolution and Mineralization of the Irtysh Fold–belt. Science Press, Beijing, p. 205 (In Chinese).

Zhao, Z.H., Wang, Z.G., Zou, T.R., Masuda, A., 1993. The REE, isotopic composition of O, Pb, Sr and Nd and petrogenesis of granitoids in Altai region. In: Tu, G.C. (Ed.), Progress of Solid-earth Science in Northern Xinjiang, China, pp. 239–266 (in Chinese with English abstract).

Zhuang, Y.X., 1993. Tectonothermal Evolution in Space and Time and Orogenic Processes of the Altaid, China. Jilin Science and Technology Press, Chuangchun, pp. 10–60 (in Chinese with English abstract).

Zou, T.R., Cao, H.Z., Wu, B.Q., 1988. Orogenic or anorogenic granitoids of the Altay Mountains, Xinjiang and their discrimination Criteria. Acta Geologica Sinica 62, 228–245 (in Chinese with English abstract).